Pergamon

Int. J. Heat Mass Transfer. Vol. 40, No. 3, pp. 699–709, 1997

0017–9310/97 $15.00 + 0.00

PII: S0017–9310(96)00146–9

Effect of finite deformations on internal heat–mass transfer in elastomer ablating materials

YU. I. DIMITRIENKO

"NPO Mashinostroeniya" R&D Industrial Corporation, Gagarina 33a, Reutov, Moscow region, 143952 Russia

(*Received* 30 *November* 1995)

Abstract—The present paper investigates a problem on modelling of internal heat–mass transfer and deforming processes in porous elastomer materials ablating under high temperatures and withstanding finite deformations (up to tens of percents). Attention is mainly paid to investigation of the effect of finite deformations on kinetics of heat transfer and mass transfer of gases in pores in the presence of an inner source of gas generation (e.g. pyrolysis of elastomer phase). It is shown that mathematical statements of the problems on internal heat–mass transfer and deforming in case of finite deformations are coupled. The following phenomena result from this coupledness: growing pore pressure of pyrolytical gases and cooling the material in mechanical compression, the appearance of tensile shrinkage stresses near the heated surfaces of the material. All the effects are investigated numerically. Copyright © 1996 Elsevier Science Ltd.

1. INTRODUCTION

Elastomer thermal-protective materials are often applied to protect load-bearing elements of structures against the action of heat fluxes. These materials are capable of work under high temperatures up to 3000°C during tens of seconds and withstanding finite deformations. These materials are very effective for thermal protection of combustion chambers of rocket solid-propellant engines and also for packing of different structural joints working under high temperatures.

Elastomer thermal-protective materials (ETPM) consist, as a rule, of an elastomer matrix ablating at high temperatures and filled in with stiff fillers to improve functional properties of the material (lowering heat-conductivity, increasing heat-stability, etc.), i.e. ETPM represent ablating composite materials.

Methods of computations for ablating materials under high temperatures and small strains are presented in refs. [1–6]. Therein the main phenomena caused by ablation in composites were investigated: the appearance of intrapore pressure of gases generating due to pyrolysis of polymer phase of the composite, the appearance of local tensile transverse stresses in shell structures made of ablating composites that leads to delamination of the shells, etc.

For elastomer thermal-protective materials, deformation of which are finite (tens of percents), internal heat–mass transfer processes have the following peculiarities: compressibility of ETPM leads to decreasing porosity and, hence, to growing intrapore pressure. This intrapore pressure of pyrolysis gaseous products redistributes a stress state of the structure of ETPM.

In the present paper computation methods for internal heat–mass transfer and thermal stresses in ablating elastomer materials with finite deformations are developed.

2. MAIN ASSUMPTIONS OF THE MODEL

Ablation processes occur in elastomer composite materials under high temperatures. These ablation processes are usually divided into: volumetric ablation (pyrolysis) and surface ablation (moving away the material from the surface). Volumetric ablation leads to decrease in density due to internal gas generation, but surface ablation causes decreasing geometrical dimensions of the structure of ETPM. Volumetric ablation is a physico-chemical process of decomposition of polymer (elastomer) phase when there occur formation of a new solid phase (pyrolytical residue) and generation of big gas quantities in pores.

Elastomer composite materials ablating under high temperatures will be considered as four-phase medium wherein:

- phase 1 is a stiff filler thermostable under considered temperatures;
- phase 2 is elastomer non-decomposed phase;
- phase 3 is a solid pyrolytical residue;
- phase 4 is a gaseous products of pyrolysis of elastomer phase.

All the solid phases ($i = 1, 2, 3$) are assumed to be incompressible in volume, but the composite itself is volumetrically compressible due to decreasing its porosity, therefore densities of solid phases are considered to be constants: $\rho_i = \text{const}$, $i = 1, 2, 3$. The

NOMENCLATURE

c, c_i	specific heat capacities [m^2 (s^2 K)$^{-1}$]
c_p	specific heat capacity of gas phase at a constant pressure [m^2 (s^2 K)$^{-1}$]
D	rate of surface ablation [m s^{-1}]
E, E_i	elasticity modules of ETPM and phases [kg (m s^2)$^{-1}$]
E_a	activation energy [m^2 (sec^2)$^{-1}$]
$\mathbf{E}$	metric tensor
$\mathbf{e}_Z$, $\mathbf{e}_R$, $\mathbf{e}_\Phi$	basis vectors of a cylindrical coordinate system
Δe_g^0, Δe_g^*	heat of volumetric and surface ablation
$\mathbf{F}$	gradient of deformations
I_e	enthalpy of a gas flow on the ablating surface [m^2 s^{-2}]
J	rate of volumetric ablation (pyrolysis) [kg (m^3 s)$^{-1}$]
L, L_i	heat-conductivity coefficients of ETPM and its phases [W (m K)$^{-1}$]
p_e'	pressure head on the internal surface of ETPM [kg (m s^2)$^{-1}$]
p	pore gas pressure [kg (m s^2)$^{-1}$]
q_e, q_R, q_{bl}, q_W	heat fluxes [kg s^{-3}]
$\mathbf{r}$	radius-vector in the initial configuration
$\mathbf{R}$	radius-vector in the actual configuration
R_a	$= 0.31$ kJ [kg K]$^{-1}$, universal gas constant
R_D	coordinate of an ablation surface [m]
$\mathbf{T}$	Cauchy stress tensor [kg (m s^2)$^{-1}$]
t	time [s]
$\mathbf{u}$	displacement vector [m]
V	volume of ETPM in the actual configuration [m^3]
$\mathbf{v}$, v_R, v_Z	velocity vector and its components in the cylindrical coordinate system [m s^{-1}].

Greek symbols

α_i	coefficients of heat phase expansion [K^{-1}]
β	shrinkage coefficient
Γ	gasification coefficient
$\mathring{\varepsilon}$	heat deformation
θ	temperature [K]
λ, μ	Lamet elasticity parameters [kg (m s^2)$^{-1}$]
Λ	Cauchy–Green strain tensor
ν	Poisson coefficient
ρ	density [kg m^{-3}]
σ_R, σ_Φ, σ_Z	stress components in cylindrical coordinate [kg (m s^2)$^{-1}$]
φ_i, φ_g	volumetric phase concentrations
ψ	free energy of ETPM [m^2 s^{-2}].

Indices

bl	indicator of parameters of outflowing gas into the surroundings
e	parameters related to the surroundings with respect to the considered domain V occupied by an ETPM
g	parameters of a gas phase
s	parameters of a solid framework.

filler is assumed to be thermo-stable, velocities of motion of all the solid phases are the same, motion of gas in pores is described by the Darcy law, heating is considered to be quasistatic so that there is a heat equilibrium of phases, therefore temperatures of all the phases are the same.

3. BASIC EQUATIONS

The equation system describing a thermo-mechanical behaviour of four-phase porous system consists of five equations of internal heat–mass transfer:

$$\frac{\partial \varphi_1}{\partial t} + \nabla \cdot \varphi_1 \mathbf{v} = 0, \tag{1}$$

$$\frac{\partial \varphi_2}{\partial t} + \nabla \cdot \varphi_2 \mathbf{v} = -\frac{J}{\rho_2}, \tag{2}$$

$$\frac{\partial \varphi_3}{\partial t} + \nabla \cdot \varphi_3 \mathbf{v} = \frac{J(1-\Gamma)}{\rho_3}, \tag{3}$$

$$\frac{\partial \rho_g \varphi_g}{\partial t} = \nabla \cdot (K \nabla p) + J\Gamma, \tag{4}$$

$$\rho_s c \frac{\partial \theta}{\partial t} = \nabla \cdot (L \nabla \theta) + c_p \varphi_g k \nabla \theta \cdot \nabla p - J \Delta e^0, \tag{5}$$

three equations of mechanical equilibrium of porous material:

$$\nabla \cdot \mathbf{T} - \nabla \varphi_g p = 0 \tag{6}$$

and three kinematic equations

$$\frac{\partial \mathbf{u}}{\partial t} + \mathbf{v} \cdot \nabla \otimes \mathbf{u} = \mathbf{v}. \tag{7}$$

Equations (1)–(4) are continuity equations for four phases, equation (5) is heat-conductivity equation of the whole elastomer material.

All the equations (1)–(7) are written in the actual configuration, i.e. they are defined within a mobile domain $V(t)$ changing its geometry due to two causes: finite deformations and surface ablation. Here ∇ is the

nabla-operator of the actual configuration $V(t)$. Let us denote $\Sigma(t)$ a surface of the domain $V(t)$ in the actual configuration.

Equation of the surface $\Sigma(t)$ at any time t has the form: $f(\mathbf{R}, t) = 0$, wherein function f is determined by the differential equation:

$$\frac{\partial f}{\partial t} + D(\nabla f \cdot \nabla f)^{1/2} + \mathbf{v} \cdot \nabla f = 0. \tag{8}$$

Volumetric concentrations of phases φ_i, φ_g are connected by the relations:

$$\varphi_g = 1 - \sum_{i=1}^{3} \varphi_i. \tag{9}$$

Herein we introduce the following notation: $\mathbf{v}$ is the velocity of solid phases, $\mathbf{u}$ is the displacement vector of solid phases, ρ_g is the density of gas in pores, φ_g is the porosity, ρ_s, c are density and heat capacity of the whole elastomer material:

$$\rho_s c = \sum_{i=1}^{3} \rho_i \varphi_i c_i, \quad \rho_s = \sum_{i=1}^{3} \rho_i \varphi_i, \tag{10}$$

where J is the mass rate of volumetric ablation (pyrolysis); D is the linear rate of surface ablation; K, L are gas-permeability and heat-conductivity coefficients of the porous elastomer material; $\mathbf{T}$ is the tensor of true Cauchy stresses in the solid frame being the collection of all solid phases; p is pore gas pressure.

4. CONSTITUTIVE RELATIONS

Elastomer material is considered to be isotropic. Constitutive relations of elastomer thermal protective material are chosen in the form of connection of Cauchy stress tensor $\mathbf{T}$ and Cauchy–Green tensor of finite deformations Λ:

$$\mathbf{T} = -p\mathbf{E} + \frac{\rho_s}{\rho_s^0} \mathbf{F}^{T-1} \cdot \frac{\partial \psi}{\partial \Lambda_\theta} \cdot \mathbf{F}^{-1}, \tag{11}$$

where the Cauchy–Green tensor Λ and inverse gradient of deformations $\mathbf{F}^{-1}$ are determined in terms of the displacement vector of the frame $\mathbf{u}$ in the following way:

$$\Lambda = \tfrac{1}{2}(\mathbf{E} - \mathbf{F}^{T-1} \cdot \mathbf{F}^{-1}), \tag{12}$$

$$\mathbf{F}^{T-1} = \mathbf{E} - (\nabla \otimes \mathbf{u})^T, \tag{13}$$

$$\Lambda_\theta = \Lambda - \mathring{\varepsilon}\mathbf{E}. \tag{14}$$

Here $\mathbf{E}$ is the unit (metric) tensor; symbol $()^T$ means transposition of a tensor; symbol $\otimes$ means a tensor product and $\mathring{\varepsilon}$ is the heat deformation of elastomer material describing heat expansion and shrinkage of the material under high temperatures:

$$\mathring{\varepsilon} = (\alpha_1 \varphi_1 + \alpha_2 \varphi_2)(\theta - \theta_0) + \frac{\alpha_3 (1 - \Gamma)}{\rho_3} \int_0^t (\theta(t) - \theta(\tau)) J \, d\tau - \beta \varphi_3. \tag{15}$$

Here α_i are the coefficients of heat expansion of solid phases; β is the shrinkage coefficient of the elastomer material under high temperatures when there occurs a volumetric ablation in the material.

Function ψ called Helmholtz free energy is chosen to be dependant on invariants of tensor Λ_θ:

$$\psi = \left(\frac{\lambda_2}{2} I_{1\theta}^2 + \mu_2 I_{2\theta} \right) a', \tag{16}$$

here $I_{1\theta}$ and $I_{2\theta}$ are the first and the second invariants of tensor Λ_θ

$$I_{1\theta} = \Lambda_\theta : \mathbf{E}; \quad I_{2\theta} = \Lambda_\theta : \Lambda_\theta, \tag{17}$$

and λ_2 and μ_2 are the Lamet elastic constants of the elastomer phase $i = 2$ connected to the Young modulus E_2 and Poisson coefficient ν by the relations:

$$\lambda_2 = \frac{\nu E_2}{(1+\nu)(1-2\nu)}; \quad \mu_2 = \frac{E_2}{2(1+\nu)}.$$

The Poisson coefficient ν is assumed to be the same for all the phases.

Function a' at normal temperature $\theta = \theta_0$ describes the ratio of elasticity constants λ, μ, E of the whole elastomer material to corresponding constants of the elastomer phase $(i = 2)$: $a' = \lambda/\lambda_2 = E/E_2$. At high temperatures function a' describes degradation of elasticity properties of elastomer material. This function a' depends on volumetric concentrations of phases:

$$a' = (1 - S_3'^2)\tilde{a} + S_3'^2 a_Q';$$

$$a_Q' = \left(\frac{1 - S_3'}{\tilde{a}} + \frac{S_3' h_c}{\kappa_1} + \frac{S_3'(1 - h_c)}{\kappa_1 h_c (2 - h_c)} \right)^{-1};$$

$$\tilde{a} = \left(\frac{S_2'}{a_p} + \frac{S_3' - S_2'}{a_Q} + \frac{1 - S_3'}{a_0} \right)^{-1};$$

$$a_p = (1 - S_3^2) a_0 + \kappa_3 (S_3^2 - S_2^2);$$

$$a_Q = (1 - S_3^2) a_0 + \kappa_3 S_3^2;$$

$$a_0 = \exp\left(-a \left(\Delta\theta + P \int_0^t \exp(-Q(t-\tau)) \, \Delta\theta \, d\tau \right)^4 \right). \tag{18}$$

Here a, P and Q are the constants determined in experiments and characterized a change of properties of polymer phase in heating, $\kappa_1 = E_1/E_2$ is the ratio of elastic constants of filler and elastomer phase, $\kappa_3 = E_3/E_2$ is the ratio of elastic constants of pyrolytic and elastomer phases. Functions S_2, S_3 and S_3' are connected to phase concentrations in the following way:

$$S_2 = \left(\frac{\varphi_g}{1 - \varphi_1} \right)^{1/3};$$

$$S_3 = \left(1 - \frac{\varphi_2}{1-\varphi_1}\right)^{1/3};$$

$$S_3' = \varphi_1^{1/3}.$$

Here h_c is the geometrical parameter characterizing a shape of the filler.

On substituting expression (16) for free energy ψ into equation (11), constitutive relations are obtained in the following form:

$$\mathbf{T} = -p\mathbf{E} + a' \frac{\rho_s}{\rho_s^0} \mathbf{F}^{T-1} \cdot (\lambda_2 I_{1\theta} \mathbf{E} + 2\mu_2 \Lambda_\theta) \cdot \mathbf{F}^{-1}. \tag{19}$$

Gas in pores is considered to be ideal and perfect, i.e.:

$$p = R_a \rho_g \theta. \tag{20}$$

5. HEAT-CONDUCTIVITY AND GAS-PERMEABILITY

Like elastic constants, heat-conductivity coefficient L of porous elastomer material depends on volumetric phase concentrations φ_i:

$$L = L_2 b', \tag{21}$$

where L_2 is the heat-conductivity coefficient of elastomer phase, and b' is the coefficient of degradation of heat-conductivity in heating:

$$b' = (1 - S_3'^2)\tilde{b} + S_3'^2 b_Q';$$

$$b_Q' = \left(\frac{1-S_3'}{\tilde{b}} + \frac{S_3' h_c}{\omega_1} + \frac{S_3'(1-h_c)}{\omega_1 h_c (2-h_c)}\right)^{-1};$$

$$\tilde{b} = \left(\frac{S_2'}{b_p} + \frac{S_3' - S_2'}{b_Q} + 1 - S_3'\right)^{-1};$$

$$b_p = 1 - S_3^2 + \omega_3 (S_3^2 - S_2^2);$$

$$b_Q = 1 - S_3^2 + \omega_3 S_3^2. \tag{22}$$

Here $\omega_1 = L_1/L_2$ and $\omega_3 = L_3/L_2$ are the ratios of heat-conductivities of the phases.

Gas-permeability coefficient K of porous thermal-protective material is determined by porosity coefficient φ_g [1]:

$$K = K_0 \exp(n\varphi_g^{1/3}), \tag{23}$$

where K_0 and n are the universal constants independent of the material type and the presence of fillers in the material.

6. ABLATION RATE

Rate of volumetric ablation (pyrolysis) J of polymer phase $i = 2$ in heating depends on temperature θ and phase content φ_2:

$$J = J^0 \varphi_2 \exp\left(-\frac{E_a}{R_a \theta}\right), \tag{24}$$

where J^0 is the pre-exponential multiplier, E_a is the activation energy.

Surface ablation of thermal-protective materials can be of different types: combustion, sublimation, melting, thermomechanical erosion etc. For ETPM, applied for thermal protection of combustion chambers, the type of thermomechanical erosion is the most typical, wherein moving away the material surface occurs due to thermomechanical destruction of substance particles of the surface.

Rate of linear ablation D occurring according to the thermomechanical type is determined by formula [1]:

$$D = \frac{1}{\rho}\left(\frac{J^0 L}{c \ln(\varphi_2^0/\varphi_{2w})}\right)^{1/2} \left(\frac{R_a \theta_w}{E_a}\right)^{1/2} \exp\left(-\frac{E_a}{2R_a\theta_w}\right). \tag{25}$$

Function φ_{2w}/φ_2^0, being the ratio of the concentration of polymer phase at initial state before heating to the concentration of polymer phase on the ablation surface in heating, is determined by the equation:

$$\frac{\varphi_{2w}}{\varphi_2^0} = 1 - \left(1 + \left(\frac{6p_e'}{\sigma}\right)^{1/2}\right)^{-3}. \tag{26}$$

Here θ_w is the surface temperature; p_e' is the pressure head on the material surface.

7. BOUNDARY CONDITIONS

At the part $\Sigma_1(t)$ of the external surface $\Sigma(t)$ of elastomer material subjected to the influence of heat fluxes q_e, boundary conditions for the system (1)–(8) are given as follows:

$$\mathbf{T} \cdot \mathbf{n} - \varphi_g p \mathbf{n} = p_e';$$

$$p = p_e', \quad \text{at } \Sigma_1(t)$$

$$-L\mathbf{n} \cdot \nabla\theta = q_e + q_{bl} - q_w - q_R. \tag{27}$$

At the surface part $\Sigma_2(t)$ of the thermal-protective elastomer material, that remains cold and is connected to a load-bearing element of the structure, boundary conditions have the form:

$$\mathbf{u} = \mathbf{u}_e, \quad \mathbf{n} \cdot \nabla p = 0, \quad \mathbf{n} \cdot \nabla\theta = 0 \quad \text{at } \Sigma_2(t). \tag{28}$$

Here $\mathbf{n}$ is the normal vector; q_{bl} is the part of the heat flux absorbed due to blowing gas from pores into the surroundings; q_w is the heat flux part absorbed due to surface ablation (for ablation of the thermomechanical type $q_w = 0$); q_R is the heat flux part rejected from the heated surface $\Sigma(t)$ due to own radiating:

$$q_{bl} = \gamma c_p K \mathbf{n} \cdot \nabla p (I_e - c\theta_w);$$

$$q_e = \left(\frac{\alpha}{c_p}\right)(I_e - c\theta_w); \quad q_R = \varepsilon\sigma\theta_w^4; \tag{29}$$

where γ is the injection coefficient ($0 < \gamma \leqslant 1$); (α/c_p) is the heat-exchange coefficient of surface $\Sigma_1(t)$ and the gas surroundings; I_e and p'_3 are enthalpy and velocity head of the overrunning flow onto the surface of ETPM, respectively; $\theta_e = I_e/c_p$ is the temperature of the flow, ε and σ are the blackness degree and the Stefan–Boltsman constant; θ_w is the temperature of the surface $\Sigma_1(t)$.

8. THE PROBLEM STATEMENT

On completing the equation system (1)–(8) by initial conditions:

$$t = 0: \quad \varphi_1 = \varphi_1^0, \quad \varphi_2 = \varphi_2^0, \quad \varphi_3 = \varphi_3^0, \quad \rho_g = \rho_g^0, \quad \mathbf{u} = 0, \quad \theta = \theta_0, \tag{30}$$

we obtain the system of 12 equations for 12 functions: φ_1, φ_2, φ_3, ρ_g, $\mathbf{u}$, $\mathbf{v}$, θ and f.

Unlike the case of small deformations considered in ref. [1], equations (1)–(7) are coupled, i.e. heat–mass transfer equations (1)–(5) and mechanics equations (6) and (7) cannot be resolved separately from each other.

9. THE PROBLEM ON ELASTOMER COATING OF A CYLINDRICAL SHELL

Let us consider a problem on determination of a stress–strain state of thermal-protective coating made of ETPM, that can be represented by a hollow cylinder fastened together with a load-bearing frame on the external surface. ETPM is subjected to the combined action of heat flux q_e supplied from the inside and internal pressure p'_e of gas filling the cylinder cavity. The external surface of ETPM is assumed to be rigidly fastened together with the load-bearing frame, and the cylinder end displacement $k_0(t)$ which can be considerable is given (Fig. 1).

The problem on the cylindrical ETPM is considered in the following axisymmetric statement. Radius r, angle φ and axial coordinate z are chosen as material coordinates. In the actual configuration, coordinates of the same material point have the values R, Φ and Z, respectively, so that radius-vectors of the point in the initial and actual configurations

$$\mathbf{r} = r\mathbf{e}_R + z\mathbf{e}_z, \quad \mathbf{R} = \mathbf{u} + \mathbf{r} = R\mathbf{e}_R + Z\mathbf{e}_Z, \tag{31}$$

are connected by the relations:

$$r = g(R, t); \quad z = \frac{Z}{k(t)}; \tag{32}$$

where $\mathbf{e}_R$, $\mathbf{e}_\Phi$ and $\mathbf{e}_Z$ are the basis vectors of the cylindrical coordinate system coinciding in the initial and actual configurations for the axisymmetric case. Expressions determined by equations (31) and (32) for the displacement vector $\mathbf{u}$, the velocity vector $\mathbf{v}$, the inverse gradient of deformations $\mathbf{F}^{-1}$ and for the strain tensor Λ and also for its invariants have the following form:

$$\mathbf{u} = (R-g)\mathbf{e}_R + Z\left(1-\frac{1}{k}\right)\mathbf{e}_Z;$$

$$\mathbf{v} = v_R\mathbf{e}_R + v_Z\mathbf{e}_Z = -\frac{1}{g'}\frac{\partial g}{\partial t}\mathbf{e}_R + \frac{Z}{k}\frac{\partial k}{\partial t}\mathbf{e}_Z;$$

$$\mathbf{F}^{-1} = \mathbf{F}^{T-1} = g'\mathbf{e}_R \otimes \mathbf{e}_R + \frac{g}{R}\mathbf{e}_\Phi \otimes \mathbf{e}_\Phi + \frac{1}{k}\mathbf{e}_Z \otimes \mathbf{e}_Z;$$

$$\mathbf{g}' \equiv \frac{\partial g}{\partial R}, \tag{33}$$

$$\Lambda = \frac{1}{2}(1-g'^2)\mathbf{e}_R \otimes \mathbf{e}_R + \frac{1}{2}\left(1-\frac{g^2}{R^2}\right)\mathbf{e}_\Phi \otimes \mathbf{e}_\Phi + \left(1-\frac{1}{k^2}\right)\mathbf{e}_Z \otimes \mathbf{e}_Z; \tag{34}$$

$$I_1 = \frac{1}{2}\left(3-g'^2-\frac{g^2}{R^2}-\frac{1}{k^2}\right);$$

$$I_2 = \frac{1}{4}\left((1-g'^2)+\frac{g^4}{R^2}+\frac{1}{k^4}\right);$$

$$I_3 = \frac{g'g}{Rk}; \quad I_{1\theta} = I_1 - 3\mathring{\varepsilon}. \tag{35}$$

Taking account of equations (19), (33) and (35), the Cauchy's stress tensor has the structure:

$$\mathbf{T} = \sigma_R\mathbf{e}_R \otimes \mathbf{e}_R + \sigma_\Phi\mathbf{e}_\Phi \otimes \mathbf{e}_\Phi + \sigma_Z\mathbf{e}_Z \otimes \mathbf{e}_Z; \tag{36}$$

where physical components of stresses σ_R, σ_Φ and σ_Z are determined by the formulae:

$$\sigma_R = -p + \frac{\rho_s}{\rho_s^0}g'^2[-(3\lambda_2+2\mu_2)a'\mathring{\varepsilon} + \lambda_2 a' I_1 + \mu_2 a'(1-g'^2)];$$

$$\sigma_\Phi = -p + \frac{\rho_s g^2}{\rho_s^0 R^2}\left[-(3\lambda_2+2\mu_2)a'\mathring{\varepsilon} + \lambda_2 a' I_1 + \mu_2 a'\left(1-\frac{g^2}{R^2}\right)\right];$$

$$\sigma_Z = -p + \frac{\rho_s}{\rho_s^0 k^2}\left[-(3\lambda_2+2\mu_2)a'\mathring{\varepsilon} + \lambda_2 a' I_1 + \mu_2 a'\left(1-\frac{1}{k^2}\right)\right]. \tag{37}$$

The equilibrium equation (6) in physical components for a cylinder of elastomer composite has the form:

$$\frac{\partial \sigma_R}{\partial R} + \frac{(\sigma_R - \sigma_\Phi)}{R} - \frac{\partial \varphi_g p}{\partial R} = 0, \quad 0 \leqslant R \leqslant R_D. \tag{38}$$

The equation to determine function $R = R_D(t)$,

describing the location of the mobile boundary changing because of finite displacements as well as the surface ablation, can be derived from equation (8), where function f has the form $f(R, t) = R - R_D(t)$:

$$\frac{\partial R_D}{\partial t} = D - \frac{1}{g'(R_D, t)} \frac{\partial g(R_D, t)}{\partial t}. \tag{39}$$

Heat–mass transfer equations (1)–(5) and kinematic equation (7) for the cylindrical coating has the form:

$$\frac{\partial \varphi_1}{\partial t} + \frac{\partial}{\partial R}(\varphi_1 v_R) = 0;$$

$$\frac{\partial \varphi_3}{\partial t} + \frac{\partial}{\partial R}(\varphi_3 v_R) = \frac{J(1-\Gamma)}{\rho_3};$$

$$\frac{\partial \varphi_2}{\partial t} + \frac{\partial}{\partial R}(\varphi_2 v_R) = -\frac{J}{\rho_2};$$

$$\frac{\partial \rho_g \varphi_g}{\partial t} = \frac{1}{R}\frac{\partial}{\partial R}\left(RK\frac{\partial p}{\partial R}\right) + J\Gamma;$$

$$\rho_c c \frac{\partial \theta}{\partial t} = \frac{1}{R}\frac{\partial}{\partial R}\left(RL\frac{\partial \theta}{\partial R}\right) + c_g \varphi_g k \frac{\partial \theta}{\partial R}\frac{\partial p}{\partial R} - J\Delta e^0;$$

$$\frac{\partial g}{\partial t} + v_R \frac{\partial g}{\partial R} = 0. \tag{40}$$

Equations (38)–(40) allow to determine eight functions φ_1, φ_2, φ_3, ρ_g, θ, g, v_R and R_D depending on two arguments: R and t. All the equations are defined within the mobile domain $R_D \leqslant R \leqslant R_e$.

Location of the external boundary of the elastomer cylindrical shell in the actual configuration is determined by the coordinate $R = R_e = \text{const}$, and location of the mobile internal boundary—by the coordinate $R = R_D(t)$. Boundary conditions at these surfaces are:

$$R = R_e: \quad g = R_e; \quad \frac{\partial \theta}{\partial R} = 0; \quad \frac{\partial p}{\partial R} = 0;$$

$$R = R_D(t): \quad \sigma_R - \varphi_g p = -p'_e;$$

$$p = p'_e; \quad -L\frac{\partial \theta}{\partial R} = q_e - q_{bl} - q_R. \tag{41}$$

Function $k(t)$ is determined from the boundary condition on the cylinder $\mathbf{u} \cdot \mathbf{n} = k_0(t)$ at $z = z_0$, then:

$$k(t) = 1 + \frac{k_0(t)}{z_0}. \tag{42}$$

Initial conditions are:

$$t = 0: \quad \varphi_1 = \varphi_1^0, \quad \varphi_2 = \varphi_2^0,$$

$$\varphi_3 = 0, \quad \rho_g = \rho_{g0}, \quad \theta = \theta_0,$$

$$R_D = R_0, \quad v_R = 0, \quad g = R. \tag{43}$$

10. CHARACTERISTICS OF ETPM

For computations we use the following values of the constants of ETPM:

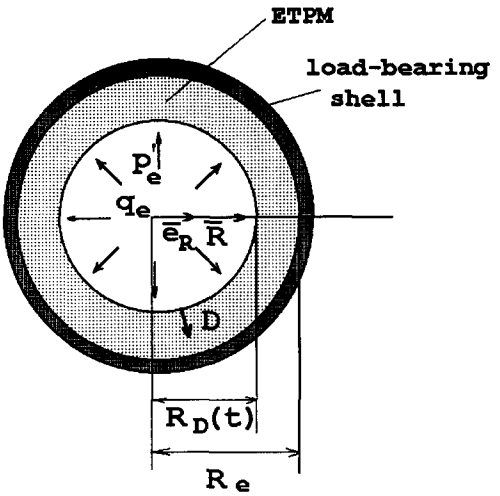

Fig. 1. A scheme of thermo-force influence of a gas-dynamical flow on a coating of a cylindrical shell made of elastomer thermal-protective material (ETPM).

$$\rho_1 = 250\,\text{kg m}^{-3}, \quad \rho_2 = 1100\,\text{kg m}^{-3},$$

$$\rho_3 = 1100\,\text{kg m}^{-3};$$

$$c_1 = 1.6\,\text{kJ(kg K)}^{-1}, \quad c_2 = 1.5\,\text{kJ(kg K)}^{-1},$$

$$c_3 = 1.5\,\text{kJ(kg K)}^{-1};$$

$$c_g = 3.1\,\text{kJ(kg K)}^{-1}, \quad L_1 = 0.1\,\text{W(m K)}^{-1},$$

$$L_2 = 0.27\,\text{W(m K)}^{-1};$$

$$L_3 = 5\,\text{W(m K)}^{-1}, \quad L_g = 0.1\,\text{W(m K)}^{-1}, \quad \Gamma = 0.6;$$

$$\alpha_1 = 2 \times 10^{-6}\,\text{K}^{-1}, \quad \alpha_2 = 20 \times 10^{-6}\,\text{K}^{-1},$$

$$\alpha_3 = 2 \times 10^{-6}\,\text{K}^{-1}, \quad \beta = 0.3;$$

$$E_1 = 70\,\text{GPa}, \quad E_3 = 0.3\,\text{GPa}, \quad \varepsilon = 0.8, \quad n = 50;$$

$$K_0 = 1.76 \times 10^{-23}\,\text{s}, \quad J^0 = 3 \times 10^5\,\text{kg(m}^{-3}\,\text{s}^{-1}),$$

$$E_a/R_a = 8 \times 10^3\,\text{K}^{-1}, \quad \varphi_1^0 = 0.2, \quad \varphi_2^0 = 0.77.$$

Elasticity modulus of polymer phase E_2 was chosen of two types: 'stiff' elastomer, $E_2 = 0.26$ GPa and 'soft' elastomer $E_2 = 0.02$ GPa. The Poisson coefficient is assumed to be equal to 0.48. Geometrical parameters of ETPM in computations were: $R_0/R_e = 0.9$.

Characteristics of heat flux in computations were chosen as follows: $c_{pe} = 2$ kJ(kg K)$^{-1}$; $(\alpha/c_p) = 4$ kg(m^2 s^{-1}); $\gamma = 0.3$.

11. COMPUTED RESULTS

Within the scope of the suggested statement, two types of thermo-force influences on elastomer material are considered (Fig. 2). The first type is characterized by the presence of relatively small pressure p'_e in the tube and by exponential growth of temperature $\theta_e(t)$. These conditions model the effect of a flame of burning substances on an elastomer fire-protective coating of a load-bearing shell. The second type of the influences

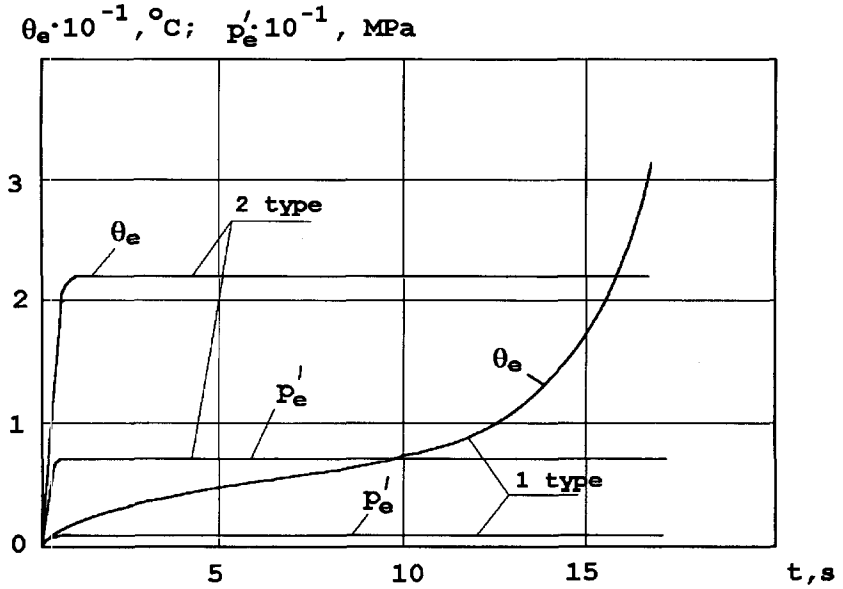

Fig. 2. Two types of thermo-force influence on ETPM used for: fire-protection of cylindrical structures (1st type) and thermal protection of structures (2nd type), where θ_e is temperature, p'_e is pressure of gas phase in the cylinder cavity.

is characterized by the presence of relatively high gas pressure p'_e (Fig. 2) and by rapid coming to a stationary regime with temperature θ_e and pressure p_e, the regime duration accounts for more than 95% of the total time of the action. These conditions model, for example, an operation of thermal-protective elastomer materials in combustors of solid-propellant engines.

Solving the problem was carried out with the help of the step-by-step method using the iterational procedures and the sweeping schemes.

To estimate the effect of finite elastomer deformations under thermo-force influence of the first type, computations for two values of the elasticity modulus $E_2 = 200$ MPa (stiff elastomer) and $E_2 = 20$ MPa (soft elastomer) were performed.

Figures 3–6 show computed temperature θ, pore pressure p and stresses σ_R and σ_Φ distributions versus the cylinder thickness for the stiff and soft materials. Let us indicate common features of the solutions for both the types. When $t \leqslant 15$ s, the intensity of heating the material is substantially less than the rate of gas products filtration through pores, that is why the pore pressure p is relatively non-high and the stresses σ_R and σ_Φ are determined only by heat expansion of the material.

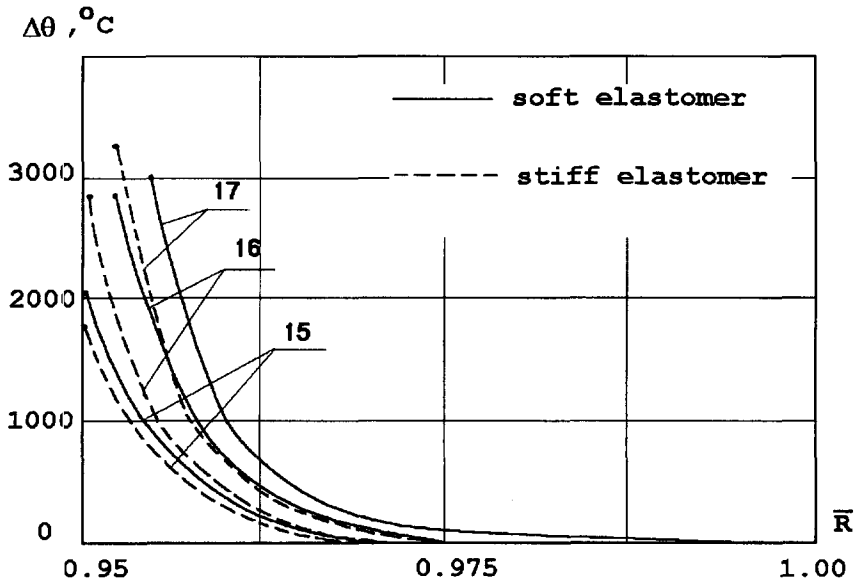

Fig. 3. Effect of elastomer stiffness on temperature distribution in a cylindrical coating, figures at curves are time t(s).

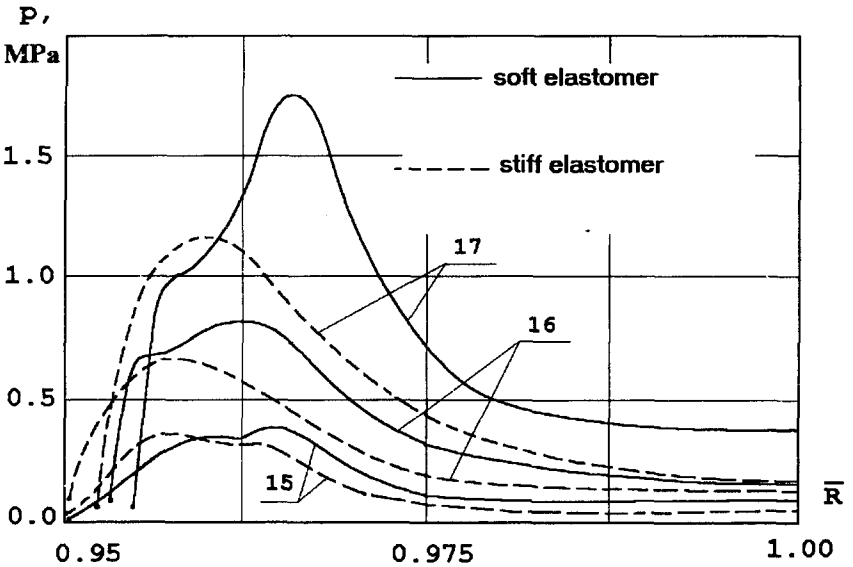

Fig. 4. Effect of elastomer ablating composite stiffness on pore pressure distribution in a cylindrical coating, figures at curves are time t(s).

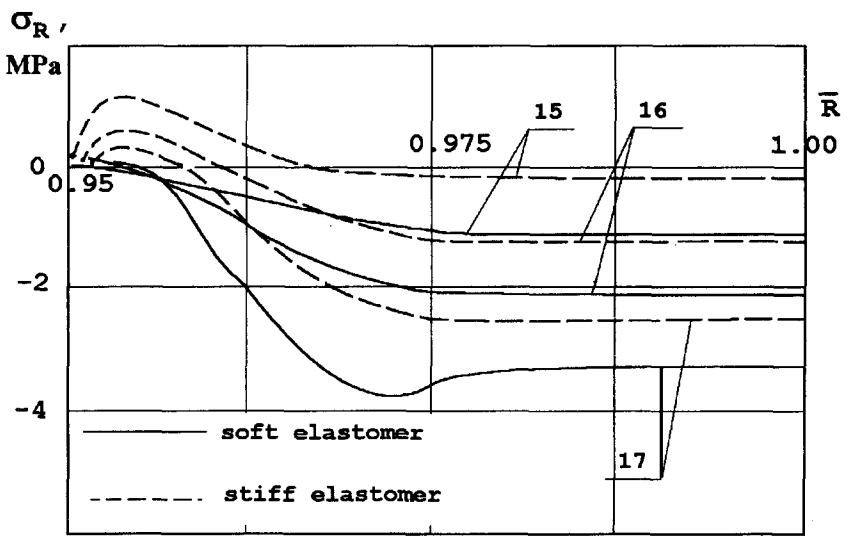

Fig. 5. Effect of elastomer ablating composite stiffness on radial stresses σ_R distribution in a cylindrical coating, figures at curves are time t(s).

There are tensile stresses σ_R at the internal surface, where the material cokes with appearance of shrinkage and there are compressing stresses σ_R and σ_Φ in the other domain due to the positive sign of heat deformation. While $t \geqslant 15$ s, pyrolysis intensity sharply increases, and gaseous products generated have no time to filtrate, therefore the pore pressure rapidly grows, begins to prevail over shrinking processes and leads to increasing the compressing stresses σ_R and σ_Φ (Figs. 5 and 6). At the internal surface, where there are pyrolysis processes, elastic features of the material considerably fall off, that is characterized by the parameter a^0.

The same time there are substantial differences in running the processes of deforming and heat–mass transfer in the stiff and soft materials. In the soft material the compressing stresses σ_R and σ_Φ lead to the considerable decrease of porosity in the cylinder zone non-heated : from $\varphi_g = 0.1$ to $\varphi_g = 0.03$. Closing the pores, in its turn, is the cause of increasing the pressure in the hot cylinder zone (Fig. 4), herein for the soft material the pressure maximum $p \approx 1.65$ MPa is higher than the one $p \approx 1.1$ MPa for the stiff material. Thanks to higher pore pressure, there are no tensile stresses in the soft material practically (Figs. 5 and 6), besides there are local maxima of compressing stresses σ_R and σ_Φ.

Although pore pressure in the stiff material is less

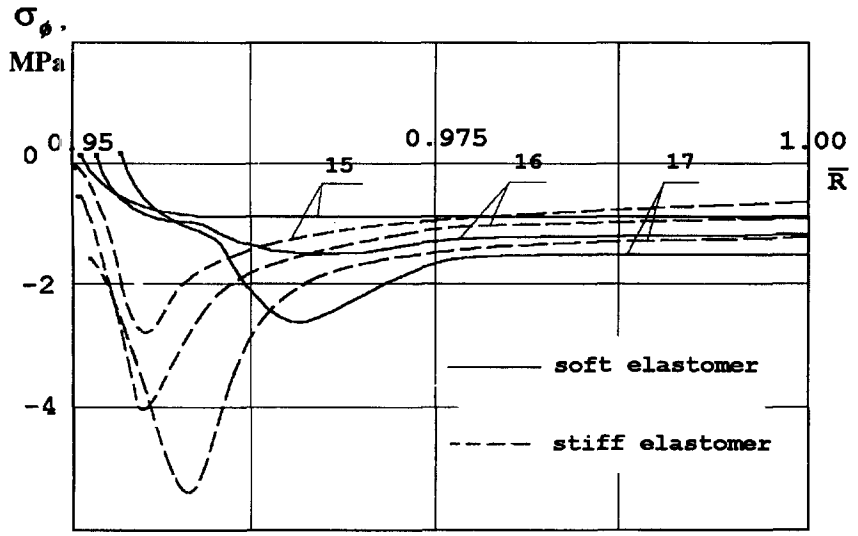

Fig. 6. Distributions of tangential stresses σ_Φ are in cylindrical coating of (1) stiff and (2) soft elastomer materials, figures at curves are time t(s).

than the one in the soft material, the absolute values of stresses σ_R and σ_Φ prove to be higher due to greater stiffness of the material.

The pore pressure increased is the cause of more intensive inner cooling the composite due to a higher rate of gas filtration to the internal surface, thus the maximal temperature of the soft material is by about 200°C lower than the one in the stiff material (Fig. 3).

Displacement of the internal boundary R_D of the soft material is more than the one for the stiff material and is equal $R_D = 0.912R_e$ and $R_D = 0.907R_e$, respectively. However, if for the stiff material this displacement occurs due only to the surface ablation, for the soft material the thickness of the material taken away is equal only to the half of the overall displacement value. The other part of the displacement is caused by deforming the material. This densifying leads to increasing the values of finite strain tensor invariants I_1 and I_2 and, hence, to increasing internal damage of the elastomer material. The phenomena above-enumerated show that finite deformations in ETPM have a considerable effect on kinetics of heat–mass transfer processes.

Let us consider now a thermo-force action of the second type. Initial porosity of elastomer material was chosen essentially less than in the first case: $\varphi_g^0 = 0.1$ and 0.03, respectively. Elasticity modulus E_2 was assumed to be equal to 60 MPa, $\nu = 0.35$, that corresponds to characteristics of a typical elastomer.

Figures 7–9 show distributions of temperature θ,

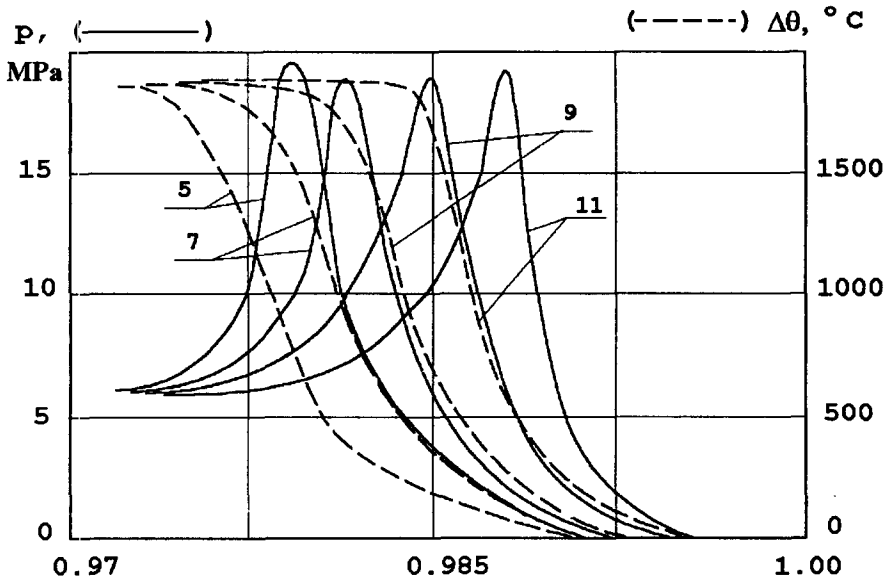

Fig. 7. Distributions of temperature $\Delta\theta$ and pore pressure p in elastomer thermal-protective coating of a cylinder under the action of internal pressure and heat flux, figures at curve are time t(s).

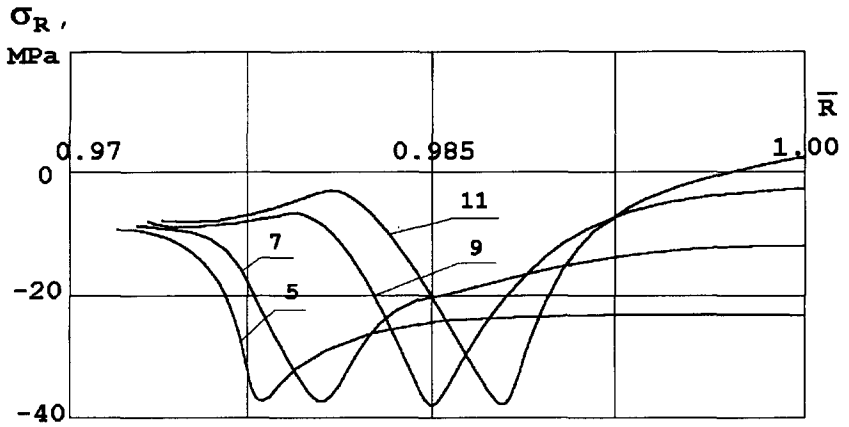

Fig. 8. Distributions of radial stresses σ_R in elastomer thermal-protective coating of a cylinder under the action of internal pressure and heat flux, figures at curves are time t(s).

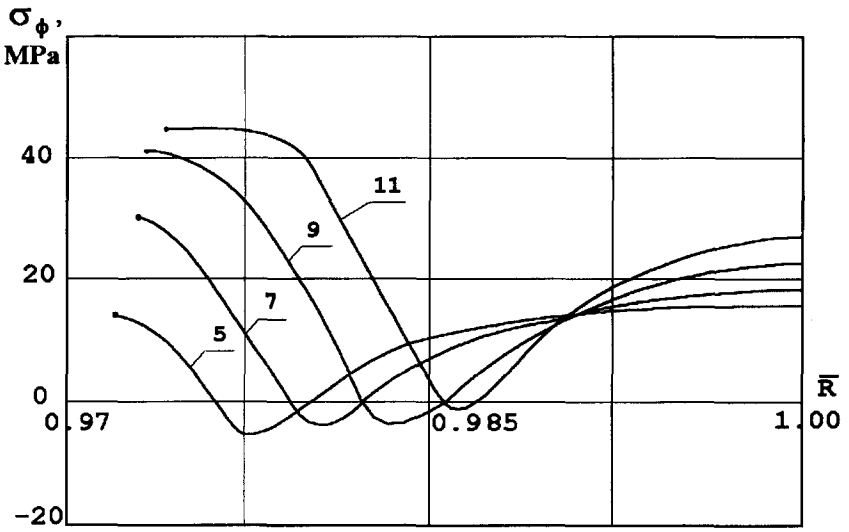

Fig. 9. Distributions of tangential stresses σ_ϕ in elastomer thermal-protective coating of a cylindrical tube under the action of internal pressure and heat flux, figures at curves are time t(s).

pore pressure p and stresses σ_R and σ_ϕ for different times of heating. In case of the action of the second type, due to essentially longer time of the influence of high temperatures than in case of the action of the first type, a considerable coked zone has time to be formed in the material, this zone being characterized by practically constant value of temperature θ (Fig. 7). A level of pore pressure is essentially higher than that for the first type, it is connected with essentially lower gas-permeability due to small porosity φ_g^0. Maximal values of p reach 15 MPa.

By a high level of internal pressure p_e' we can explain that radial stresses σ_R prove to be only compressing (Fig. 8). Therefore for the given combination of the material, the structure and the thermo-force action conditions, tangential stresses σ_ϕ are the most dangerous. At intensive pyrolysis process shrinkage tensile stresses σ_ϕ appear in the coked zone (Fig. 9); their magnitudes are rather high max $\sigma_\phi \approx 43$ MPa.

It is the tangential tensile stresses σ_ϕ that become the cause of destruction of the material in the coked zone, when strength properties of the material fall down under the limiting values.

12. CONCLUSIONS

The present paper gives the statement of the coupled problem on deforming and internal heat–mass transfer of elastomer ablating materials with finite deformations. The suggested system of equations allows to determine stress, temperature and pore pressure fields in porous reacting materials withstanding finite deformations (up to tens of percents), for example, in elastomer thermal-protective coatings of combustors of rocket engines, solid propellants (energetic materials), etc.

The conducted computations showed that finite deformations of the material have a rather considerable effect on processes of internal heat–mass transfer in such porous materials. Due to compressibility of the material its porosity changes and, hence, gas pore pressure and temperature change too,

that, in turn, redistribute internal stresses in the material. For cylindrical coatings made of elastomer ablating materials with finite deformations the appearance of local extrema of tensile stresses near the heated surface and compressing stresses in the material depth within the zone of intensive pyrolysis is typical.

Acknowledgements—The research described in this publication was made possible in part by grant no. RNB300 from the International Science Foundation.

REFERENCES

1. Yu. I. Dimitrienko, Thermal stresses and heat–mass transfer in ablating composite materials, *Int. J. Heat–Mass Transfer* **38,** 139–146 (1995).
2. Yu. I. Dimitrienko, G. A. Efremov and I. S. Epifanovski, Reusable re-entry vehicles with reclaimable ablating thermal protection. *Proceedings of 19th Int. Symp. on Space Technology and Science*, Yokohama, Japan (1994).
3. Yu. I. Dimitrienko, Ultra-light thermal protective composite materials, *Proceedings of Int. Conf. on Composite Engineering* (ICCE/2), New Orleans, pp. 189–190 (1995).
4. Yu. I. Dimitrienko and I. S. Epifanovski, Deforming and strength of ablating thermal-protective materials under high temperatures, *Mech. Compos. Mater.* **3,** 460–468 (1990) (in Russian).
5. H. N. McManus and G. S. Springer, High temperature thermo-mechanical behaviour of carbon–phenolic and carbon–carbon composites, *J. Compos. Mater.* **26,** 206–229, 230–255 (1992).
6. J. K. Chen, A. Perea and F. A. Allalhdadi, Laser effects on the dynamic response of laminated composites, *J. Compos. Engng* **5,** 1135–1147 (1995).